molecular pharmaceutics

ARTICLE

pubs.acs.org/molecularpharmaceutics

Calcium Condensed LABL-TAT Complexes Effectively Target Gene Delivery to ICAM-1 Expressing Cells

Supang Khondee,[†] Abdulgader Baoum,[†] Teruna J. Siahaan,[†] and Cory Berkland*[,†,‡]

[†]Department of Pharmaceutical Chemistry and [‡]Department of Chemical and Petroleum Engineering, The University of Kansas, Lawrence, Kansas 66047, United States

ABSTRACT: Targeted gene delivery using nonviral vectors is a highly touted scheme to reduce the potential for toxic or immunological side effects by reducing dose. In previous reports, TAT polyplexes with DNA have shown relatively poor gene delivery. The transfection efficiency has been enhanced by condensing TAT/DNA complexes to a small particle size using calcium. To explore the targetability of these condensed TAT complexes, LABL peptide targeting intercellular cell-adhesion molecule-1 (ICAM-1) was conjugated to TAT peptide using a polyethylene glycol (PEG) spacer. PEGylation reduced the transfection efficiency of TAT, but TAT complexes targeting ICAM-1 expressing cells regained much of the lost transfection efficiency. Targeted block peptides properly formulated with calcium offer promise for gene delivery to ICAM-1 expressing cells at sites of injury or inflammation.

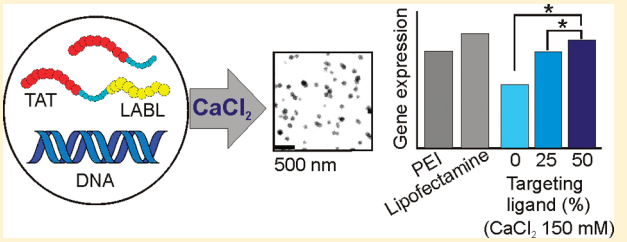

KEYWORDS: TAT, LABL, targeted gene delivery, calcium, ICAM-1

1. INTRODUCTION

The efficient delivery of therapeutic genes to a target site is a key to success in gene therapy. Viruses are very efficient gene vectors, but safety concerns such as immunogenicity of viral proteins and risk of oncogenesis still remain.[1] Nonviral vectors are continually under development and offer the potential for clinical application.[2] Cell penetrating peptides (CPPs), also called protein transduction domains (PTD), have emerged as a valuable component of nonviral vehicles facilitating the delivery of various molecules such as small molecule drugs,[3,4] imaging agents,[5,6] peptides,[7,8] proteins,[9,10] nucleic acids,[11,12] and nanoparticles[13,14] across biological barriers. CPPs are relatively short (<30 amino acids) and usually contain multiple basic amino acids. The cationic properties of many CPPs allows complexation with nucleic acids, which can be further condensed into small nanoparticles by the addition of calcium chloride.[15,16] When translating these cationic complexes to in vivo studies, shielding with polyethylene glycol (PEG) and adding a peptide ligand to enable cell targeting may improve performance.

The HIV-1 trans-activating transcriptor (TAT) protein was among the first found to be capable of translocating cell membranes and gaining intracellular access. Specific peptide domains were identified from this protein that maintained translocation ability. One specific domain, TAT_{49-57} (RKKRRQRRR), is one of the most widely studied CPPs for intracellular therapeutic delivery. TAT has been extensively utilized to deliver a multitude of cargo in liposomes, polyplexes, solid lipid nanoparticles or other nanoparticle types or by direct conjugation to molecules of interest.[17−22] TAT peptide has also been used to form electrostatic complexes with DNA and siRNA to facilitate intracellular delivery. Unfortunately, transfection efficiency of TAT complexes with DNA has been relatively poor, possibly due to an inability to form small complexes or deactivation of this CPP when bound to nucleic acids.[23,24] It has been suggested that high molecular weight cationic polymers offer stable complexes, while small polymers give rise to large, unstable complexes.[24] As a result, many groups have attempted to improve transfection efficiency by using a reducible TAT polymer[23] or by stringing together multiple TAT copies (e.g., TAT_2, TAT_3, and TAT_4).[25,26] Recent work showed that TAT/DNA complexes have comparable transfection efficiency to polyethylenimine (PEI) when condensed using calcium.[15] Calcium was reported to bind both DNA phosphate groups and/or TAT amine groups resulting in compact complexes with optimal DNA release.[15] Translation of these complexes may require charge shielding to avoid clearance or targeting to promote accumulation at diseased tissue.

Cell adhesion molecules play an essential role in cell trafficking in the immune system. Intercellular cell-adhesion molecule-1 (ICAM-1), a member of the immunoglobulin superfamily, promotes cell adhesion in immunological and inflammatory reactions. It is constitutively expressed on some tissues and upregulated by inflammatory cytokines such as interleukin-1 (IL-1), tumor necrosis factor-α (TNF-α) or interferon-γ (INF-γ).[27,28] ICAM-1 can be expressed on vascular endothelial cells, epithelial cells, fibroblasts, tissue macrophages, and antigen presenting cells.[29] The upregulation of ICAM-1 is associated with diverse diseases such as atherosclerosis, ischemia and repurfusion, asthma, arthritis, graft rejection, and cancer metastasis.[30,31] As a result, elevated ICAM-1 has been used as a target to deliver enzymes,

Received: November 18, 2010
Accepted: April 7, 2011
Revised: February 22, 2011
Published: April 07, 2011

nanoparticles, contrast agents, and antisense oligoneucleotides in an effort to improve the health of pateints.[32−38]

LABL peptide (ITDGEATDSG) is derived from the I-domain of the α_L-subunit of leukocyte function associated antigen-1 (LFA-1). LABL inhibits LFA-1/ICAM-1 interaction by binding to the D1 domain of ICAM-1 through its active region, ITDGEA.[39] Blocking ICAM-1/LFA-1 interactions with antibodies and LABL-antigenic peptide conjugate have been shown to modulate disease severity and progression of psoriasis and experimental autoimmune encephalomyelitis (EAE), a model for multiple sclerosis.[29,40−42] In addition to receptor binding, LABL can be internalized by ICAM-1 suggesting an alternative mechanism to deliver therapeutics into cells having elevated ICAM-1 expression.[43] Recent work showed that cLABL-conjugated nanoparticles could be successfully delivered to lung carcinoma epithelial cells.[32]

The aim of this study was to target TAT/DNA complexes as a means to transfect ICAM-1 expressing cells. TAT peptide was conjugated with LABL peptide using a polyethylene glycol (PEG) spacer. This block peptide was then complexed with plasmid DNA encoding luciferase. Calcium chloride was used to condense the complexes, thus yielding a small size with optimized DNA release.[15] At optimal calcium concentration, the TAT-PEG-LABL was able to target DNA to ICAM-1 expressing cells and enhance transfection in comparison to untargeted complexes (e.g., TAT-PEG) offering an effective gene carrier to ICAM-1 expressing cells.

2. MATERIALS AND METHODS

Materials. Branched polyethylenimine (PEI, 25 kDa) was purchased from Aldrich. Peptide conjugates were synthesized in house via solid phase peptide synthesis using an automated Pioneer Peptide Synthesizer (PerSeptive Biosystems, Foster City, CA). Resins were purchased from Applied Biosystems (Foster City, CA). Fmoc-$(CH_2CH_2O)_{12}$ (MW 840, 46.5 Å spacer) and Fmoc amino acids were purchased from Peptide International Inc. (Louisville, KY) and Advanced ChemTech (Louisville, KY), respectively. All peptide conjugates were purified by semipreparative HPLC on a C18 column, and the purity was determined by analytical HPLC with detection at a wavelength of 220 nm (Shimadzu scientific instruments, Columbia, MD). The molecular weight was confirmed by electron spray mass spectrometry (LCT premier mass spectrometer, Water, Milford, MA). Carcinoma human alveolar basal epithelial cells (A549) were purchased from the American Type Culture Collection (ATCC) and cultured according to ATCC protocol. Plasmid DNA encoding firefly luciferase (pGL3, 4.8 kbp) was obtained from Promega (Madison, WI). Plasmids were grown in *Escherichia coli* cells in Luria Bertani (LB) broth supplemented with 60 μg/mL ampicillin and purified using QIAGEN plasmid Giga Kits (Valencia, CA) according to the manufacturer's instructions. The DNA purity level was determined by UV/vis spectrometer. DNA with an A_{260}/A_{280} ratio of 1.8 or greater was used. F-12K medium was purchased from Mediatech, Inc. (Manassas, VA). Agarose was purchased from Fisher Scientific (Fair Lawn, NJ). Heparin sodium was obtained from Spectrum Chemical Mfg. Corp. (Gardena, CA). Recombinant, human, tumor necrosis factor-α (TNF-α), luciferase assay kit and CellTiter 96 Aqueous nonradioactive cell proliferation assay (MTS) were purchased from Promega (Madison, WI). Bicinchoninic acid assay (BCA) was purchased from Thermo Fisher Scientific Inc. (Rockford, IL). Monoclonal anti-human CD54 (ICAM-1) domain D1 and monoclonal anti-human CD54 (ICAM-1) domain D1/FITC were purchased from Ancell (Bayport, MN). Lipofectamine 2000, 4′,6-diamidino-2-phenylindole, dilactate (DAPI, dilactate), TOTO-3 and SYBR green I were purchased from Invitrogen Molecular Probes Inc. (Carlsbad, CA).

Methods. *Complex Formation.* Complex formation was conducted as described earlier.[15] Briefly, complexes were prepared by adding 10 μL (0.1 μg/μL) of DNA to 15 μL of PEI (polymer nitrogen to DNA phosphate (N/P) ratio of 10) or to 15 μL of TAT conjugates (at desired N/P ratios) followed by intensive pipetting. Fifteen microliters of DNase free water or known concentrations (e.g., 150 mM) of $CaCl_2$ solution was then added to PEI and TAT complexes respectively, and the solution was vigorously pipetted again. Complexes were allowed to incubate at 4 °C for 30 min before use. Lipofectamine/DNA complex was prepared according to the manufacturer's protocol.

Size and Morphology. Complexes were prepared as described earlier. Hydrodynamic diameters of complex solutions were determined at 20 °C by dynamic light scattering (DLS) using a DynaPro plate reader (Wyatt Technology, Santa Barbara, CA). Complexes were analyzed in Corning 384-well UV-transparent plates using 30s data acquisitions and autoattenuation laser power. The Dynamics Software package version 6.12 was used to analyze the data.

Complex size was also examined over time in serum-free F12K medium. Complexes were prepared and diluted with the medium in the same manner as in transfection study, 1 part of complex solution:4 parts of medium. Complex size was monitored at 0, 1, 2, and 4 h using a plate reader DLS.

Complexes intended for transmission electron microscopy (TEM) were air-dried on copper grids coated with carbon film. TEM images of complexes were obtained using A JEOL 1200 EXII transmission electron microscope operating at an accelerating voltage of 80 kV.

Agarose Gel Electrophoresis. Complexes were prepared as described earlier, and then 4 μL of Tris-acetate-EDTA (TAE) buffer and 4 μL of SYBR Green I were added into the mixture. The mixture was incubated at room temperature for 30 min, and 7 μL of DNA loading buffer was added. Then, 6 μL of the mixture was loaded onto a 1% agarose gel, and electrophoresed at 110 V for 30 min. A 1 kb DNA ladder was used as a marker. DNA migration bands were visualized and photographed with an Alpha Imager (Alpha Innotech Corp., San Leandro, CA).

For heparin displacement studies, complexes were challenged with 0.05 to 0.35 U of heparin for 30 min at room temperature. Complex solutions were treated with TAE buffer and SYBR Green I, followed by the addition of DNA loading buffer and electrophoresis as described above. Uncomplexed and untreated DNA diluted with identical electrophoresis solutions was used as control.

Cytotoxicity Assay. Cytotoxicity of TAT conjugates and PEI was determined using a CellTiter 96 AQ_{ueous} Cell Proliferation assay kit. A549 cells were seeded in 96-well plates (8000 cells/well) for 24 h prior to use. The growth medium was replaced with serum-free medium containing TAT conjugates and PEI at various concentrations and incubated for 24 h. After incubation, the medium containing sample was replaced with 100 μL of serum-free medium. Then, 20 μL of solution mixture of MTS ([3-(4,5-dimethylthiazol-2-yl)-5-(3-carboxymethoxyphenyl)-2-(4-sulfophenyl)-2*H*-tetrazolium]) and PMS (phenazine

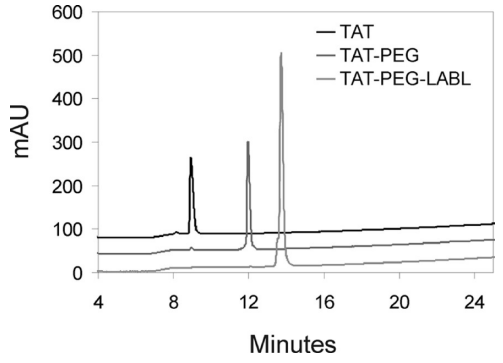

Figure 1. HPLC chromatograms for TAT, TAT-PEG, and TAT-PEG-LABL confirmed purity > 95%.

methosulfate) were added to each well, and the plates were then incubated at 37 °C, 5% CO_2 for 2 h. The absorbance of formazan product was measured at 490 nm using a microplate reader (SpectraMax M5; Molecular Devices Corp., CA).

Relative ICAM-1 Expression on A549 Cells. Cells were incubated with TNF-α (1000 U/mL) for 24 and 48 h to activate ICAM-1 expression on the cell surface.[44] Cells were then trypsinized, centrifuged, and washed three times with ice-cold PBS. Cells were divided into microcentrifuge tubes (5×10^5 cells/50 μL). AB serum was added to block nonspecific binding (25 μL) and incubated on ice for 10 min at room temperature. Cells were washed with ice-cold PBS, and monoclonal anti-human CD54 (ICAM-1) domain D1/FITC (80 μL) was added and incubated on ice for 45 min. Cells were washed three times with ice-cold PBS and fixed with 4% paraformaldehyde. The fluorescent intensity of cells was measured using the FACscan flow cytometer. Data analysis was performed using Cell Quest software (BD).

Transfection Studies. A549 cells were seeded in 96-well plate (8000 cells/well) for 24 h prior to transfection or activation of ICAM-1. Cells were incubated with TNF-α (1000 U/mL) for an additional 48 h for transfection studies on cells with upregulated ICAM-1. Complexes were prepared as described earlier. Prior to transfection, growth medium was removed and cells were washed with PBS (100 μL) twice. Complexes (20 μL) were diluted with serum-free medium (80 μL) and then were added to each well. After 5 h of transfection, transfection medium was replaced with growth medium and cells were incubated for another 48 h. The luciferase assay kit was used to determine gene expression. Cells were harvested and luciferase expression was measured according to the manufacturer's protocol. Luciferase activity was quantified in relative light units (RLUs) using a microplate reader (SpectraMax M5; Molecular Devices Corp., CA), and normalized by total cellular protein which was determined using a bicinchoninic acid (BCA) assay.

Transfection parameters such as $CaCl_2$ concentrations (0−300 mM) and N/P ratios (5−30) were optimized using TAT and TAT-PEG complexes in normal A549 cells. For targeting studies in cells activated using TNF-α, 25 and 50% of the TAT-PEG-LABL were selected to be incorporated into complexes (the remainder was TAT-PEG). Previous work demonstrated that increasing ligand density (e.g., from 25% to 50%) increased the binding and uptake of particles targeting ICAM-1 receptors.[45] Particles with 50% targeting ligand showed the highest interaction compared to other formulations. Increasing

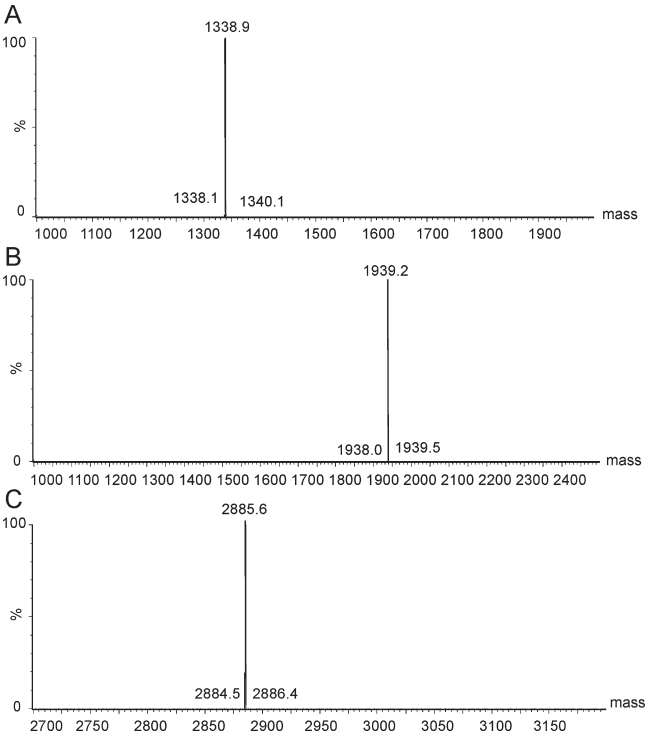

Figure 2. Electrospray ionization (ESI) mass spectra of (A) TAT, (B) TAT-PEG, and (C) TAT-PEG-LABL were in agreement with calculated masses.

ligand density (e.g., 75% and 100%) resulted in decreased binding and uptake of the particles.

The effect of ICAM-1 receptor blocking on transfection efficiencies of targeted complexes was also examined. Activated cells were incubated with various concentrations of free LABL peptide or anti-ICAM-1 mAb for 30 min. Cells were then washed three times with serum-free medium and incubated with 50% TAT-PEG-LABL/DNA and TAT/DNA complexes for 5 h. Luciferase expression was measured as described above.

Confocal Microscopy of Internalization. DNA was fluorescently labeled with the intercalating nucleic acid stain TOTO-3 using a molar ratio of 1 dye molecule per 300 base pairs for 30 min at room temperature in the dark. Then, complexes were prepared as described earlier with the labeled DNA. A549 cells activated with TNF-α mounted onto glass slides were incubated with complexes for 4 h. Cells were then washed three times with ice-cold PBS and fixed with 4% paraformaldehyde. Nuclei were labeled with DAPI dilactate (300 nM, ex 358 nm, em 461 nm) for 5 min at 37 °C, 5% CO_2. Cells were observed using an Olympus spinning disk confocal microscope and TIRF-M inverted fluorescence microscope using 20× or 60× objectives (DAPI, ex 387 nm, em 415−470 nm; TOTO-3, ex 628 nm, em 669−726 nm). Bright field transmission images were obtained at the same time.

Statistic Analysis. GraphPad Prism 4 software was used for statistical analysis. Statistical significance for differences between two data sets was determined by unpaired Student's *t*-test (90% confidential interval). One-way ANOVA, Tukey post test was used to analyze the differences when more than two data sets were compared.

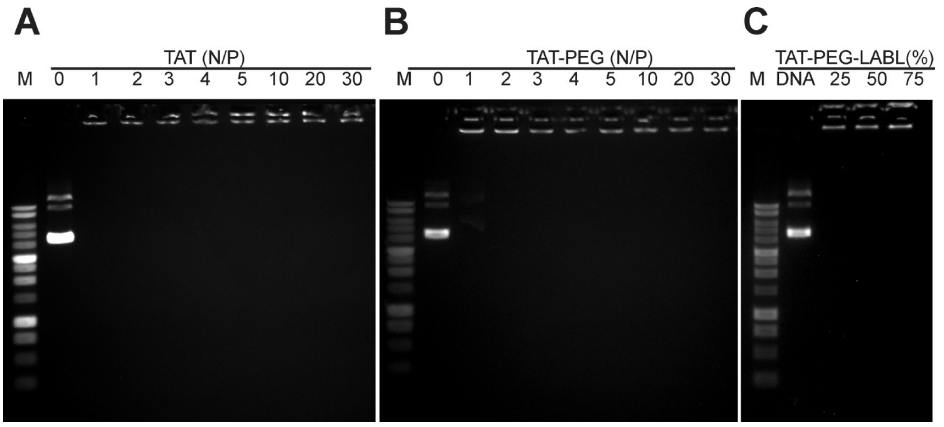

Figure 3. Gel electrophoresis of (A) TAT/DNA and (B) TAT-PEG/DNA complexes at different N/P ratios. (C) TAT-PEG-LABL/DNA complexes at an N/P ratio of 30 with different amounts of TAT-PEG-LABL combined with TAT-PEG. All complexes at all N/P ratios limited the mobility of DNA.

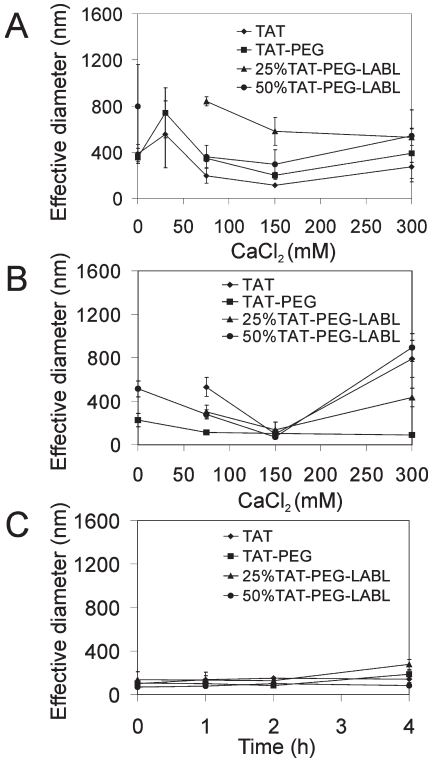

Figure 4. DLS was used to determine the size of TAT/DNA, TAT-PEG/DNA, 25% TAT-PEG-LABL/DNA, and 50% TAT-PEG-LABL/DNA complexes at an N/P ratio of 30 with different concentration of $CaCl_2$. (A) The hydrodynamic diameter of complexes were determined in deionized water and (B) in serum-free F12K media. (C) The hydrodynamic diameter of complexes (formed with 150 mM $CaCl_2$) in F12K media were stable over time. For missing data points, diameter was >1 μm.

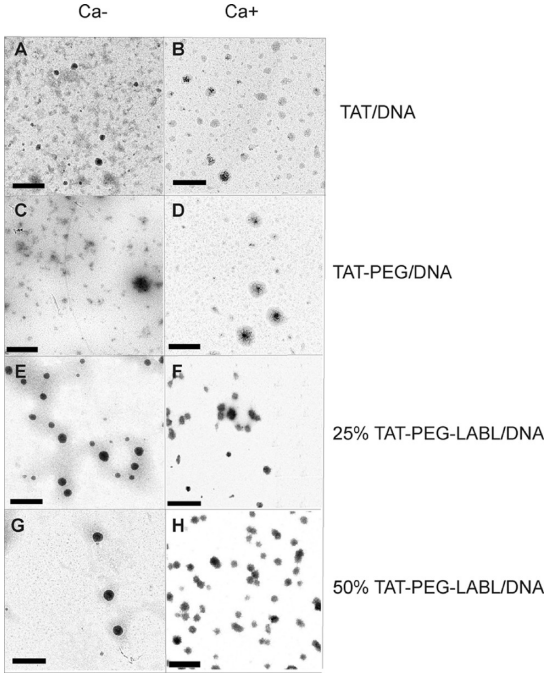

Figure 5. Transmission electron micrographs of (A) TAT/DNA, (B) TAT/DNA-Ca, (C) TAT-PEG/DNA, (D) TAT-PEG/DNA-Ca, (E) 25% TAT-PEG-LABL/DNA, (F) 25% TAT-PEG-LABL/DNA-Ca (G) 50% TAT-PEG-LABL/DNA, and (H) 50% TAT-PEG-LABL/DNA-Ca complexes. Complexes were formed at an N/P ratio of 30 without $CaCl_2$ (left panel) or with 75 mM of $CaCl_2$ (right panel). Scale bars are 500 nm.

3. RESULTS

3.1. Purification and Characterization of TAT, TAT-PEG, and TAT-PEG-LABL. All TAT peptide conjugates were synthesized according to a standard Fmoc protocol. The crude peptide and conjugates were purified by semipreparative HPLC on a C18 column, and the purity was determined by analytical RP-HPLC (purity > 95%) (Figure 1). The expected molecular weight was confirmed by electrospray ionization mass spectrometry; TAT MW 1338.9 Da, TAT-PEG MW 1939.2 Da, TAT-PEG-LABL MW 2885.6 Da (Figure 2).

3.2. Physicochemical Characterization of Complexes. An important characteristic for efficient gene delivery using cationic polymers is the formation of small and stable complexes with DNA.[46] The ability of TAT and TAT conjugates to form complexes with DNA was studied using agarose gel electrophoresis at N/P ratios of 0, 1, 2, 3, 4, 5, 10, 20, and 30. The immobilization of DNA suggested that TAT and TAT-PEG conjugates were able to form complexes with DNA and completely immobilize DNA starting at an N/P ratio of 1 and 2,

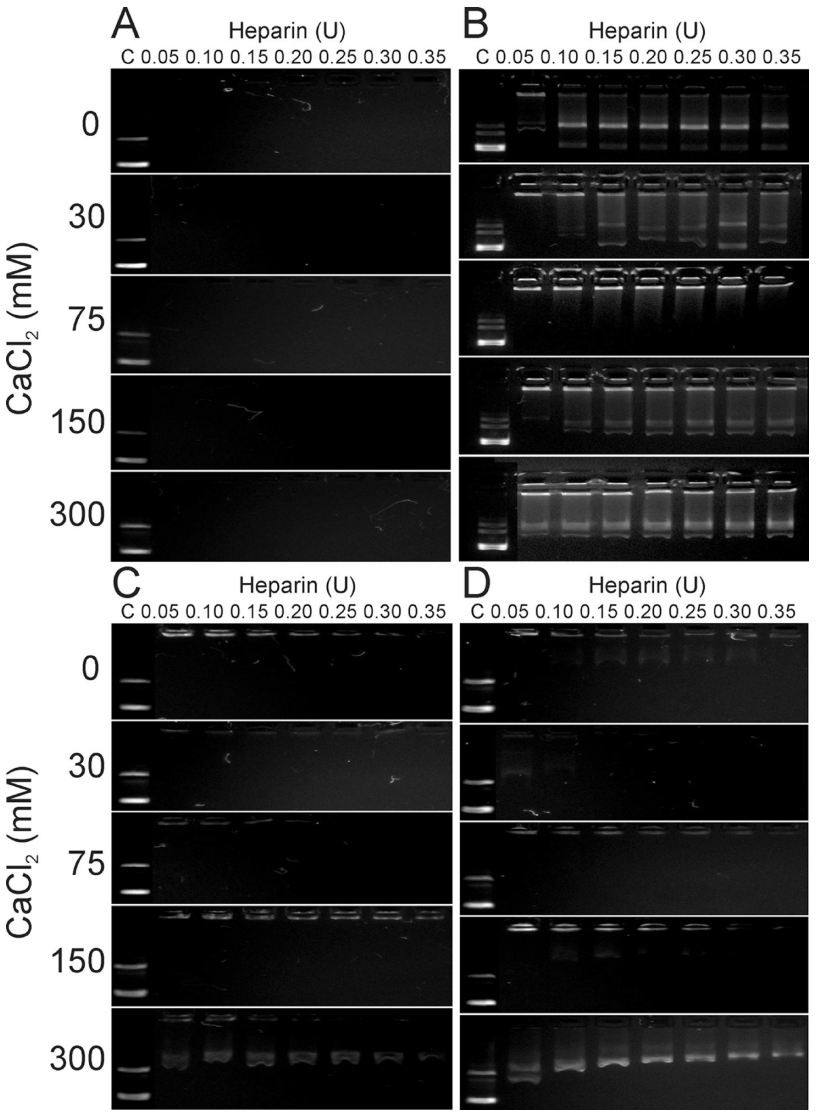

Figure 6. A heparin displacement assay for (A) TAT/DNA, (B) TAT-PEG/DNA, (C) 25% TAT-PEG-LABL/DNA, and (D) 50% TAT-PEG-LABL/DNA complexes was used to assess the effect of calcium chloride concentration (0, 30, 75, 150, 300 mM) on complex stability. Complexes were formed at an N/P of 30 and incubated for 30 min with increasing heparin concentrations (0.05−0.35 U). Free DNA is shown as a control (C) to the left.

respectively (Figure 3). Targeting ligands (TAT-PEG-LABL) were included at various ratios with TAT-PEG, and DNA mobility was assessed at an N/P ratio of 30. Targeted TAT conjugates in all formulations (e.g., 25, 50, and 75% TAT-PEG-LABL) were able to immobilize DNA. The data also suggested that PEGylation did not negatively affect the ability of TAT to complex with DNA at N/P ratios ≥ 2.

Next, hydrodynamic diameters and morphology of the complexes were evaluated by DLS and TEM, respectively. TAT, TAT-PEG, 25% TAT-PEG-LABL, and 50% TAT-PEG-LABL complexes were prepared at an N/P ratio of 30 and in the presence of various concentrations of $CaCl_2$. Complexes with discrete percentages of targeting ligands were prepared by varying the relative amounts of TAT-PEG and TAT-PEG-LABL (e.g., 25% or 50% TAT-PEG-LABL). The complex size in deionized water varied with $CaCl_2$ concentration (Figure 4A). TAT and TAT-PEG complexes were generally smaller than 25% and 50% TAT-PEG-LABL complexes. Without $CaCl_2$, most complexes were quite large (>400 nm) as determined by DLS. When adding 30 mM $CaCl_2$, the complexes were larger than the initial size suggesting that a low concentration of $CaCl_2$ may induce aggregation. Adding 150 mM $CaCl_2$ yielded a minimum diameter for most complexes (110, 190, 290 nm for TAT, TAT-PEG, and 50% TAT-PEG-LABL complexes, respectively). The data suggested that the TAT peptide could not condense DNA well without calcium chloride and that an optimal amount of calcium chloride is essential to form compact particles. Comparing the size of TAT and TAT-PEG complexes suggested that PEGylation increased the hydrodynamic diameter as observed by others.[47]

Complex size in serum-free F12K media was also determined over time. TAT, TAT-PEG, 25% TAT-PEG-LABL, and 50% TAT-PEG-LABL complexes were prepared as described earlier at an N/P ratio of 30 and in the presence of various concentrations of $CaCl_2$. Complexes were handled similarly to transfection studies. Generally, most complexes in media (Figure 4B) were substantially smaller than in deionized water (Figure 4A). At lower or higher $CaCl_2$ concentration (75 and 300 mM), particle size was initially larger than at $CaCl_2$ 150 mM, but no precipitation

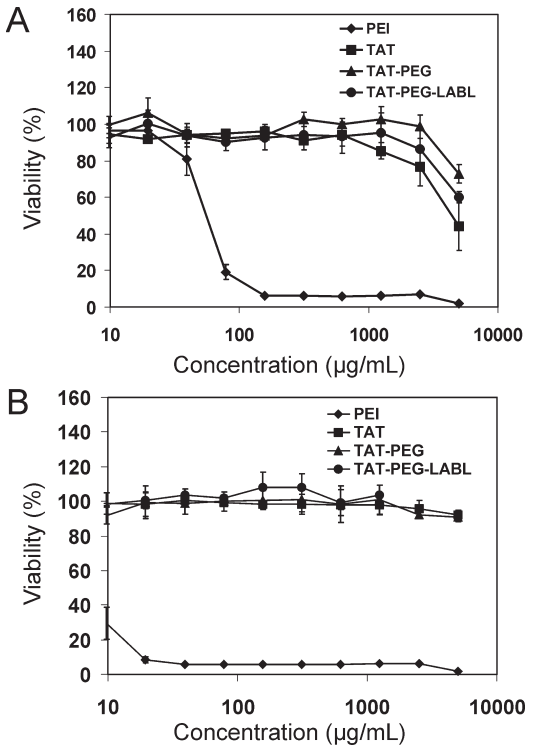

Figure 7. TAT peptide and derivatives showed low cytotoxicity in comparison to PEI (A) in unactivated and (B) in activated A549 cells, which overexpress ICAM-1.

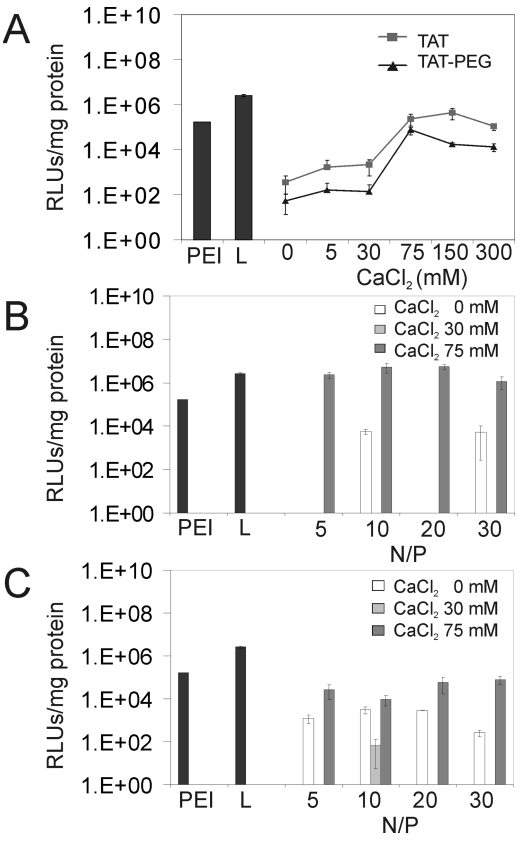

Figure 8. Transfection efficiencies of TAT peptide derivative/DNA complexes in A549 cells. (A) TAT/DNA and TAT-PEG/DNA complexes at an N/P ratio of 30 with different concentrations of calcium chloride. (B) TAT/DNA complexes at different N/P ratios. (C) TAT-PEG/DNA complexes at different N/P ratios. L = Lipofectamine.

was observed (Figure 4B). The hydrodynamic diameter was also monitored for complexes with 150 mM of added $CaCl_2$ for 4 h. Complexes were small and stable over time (Figure 4C).

The morphology of complexes was characterized using transmission electron microscopy (TEM). TAT, TAT-PEG, 25% TAT-PEG-LABL, and 50% TAT-PEG-LABL complexes were prepared as described earlier at an N/P ratio of 30. Formulations without $CaCl_2$ were compared to those including 75 mM $CaCl_2$. TEM images indicated that most complexes had a globular shape and were substantially smaller than 300 nm (Figure 5), but images reflect the dry state. Agglomerates were occasionally visible in these samples and may account for the larger diameters observed by DLS or may be attributable to sample drying. This difference between the DLS data and TEM data could be due to small amount of flocculates observed from DLS experiments. The flocculates (~1 μm, <5% of population) have greatly shifted the mean diameter, which is a major disadvantage of DLS.

Forming complexes with polycations can protect DNA from degradation and often effectively condenses DNA, but DNA release is also crucial for enhancing transfection efficiency.[48] Complex stability was evaluated by displacing DNA using heparin. TAT, TAT-PEG, 25% TAT-PEG-LABL and 50% TAT-PEG-LABL complexes were tested in this experiment. The complexes were formed at an N/P ratio of 30 using various concentrations of $CaCl_2$ and challenged with free heparin (Figure 6). TAT complexes yielded the most stable DNA complexes, whereas TAT-PEG complexes had the lowest stability. The 25% TAT-PEG-LABL and 50% TAT-PEG-LABL complexes showed intermediate stability between TAT and TAT-PEG complexes. At all $CaCl_2$ concentrations, TAT complexes were very stable and did not release DNA even at high heparin concentration (Figure 6A).

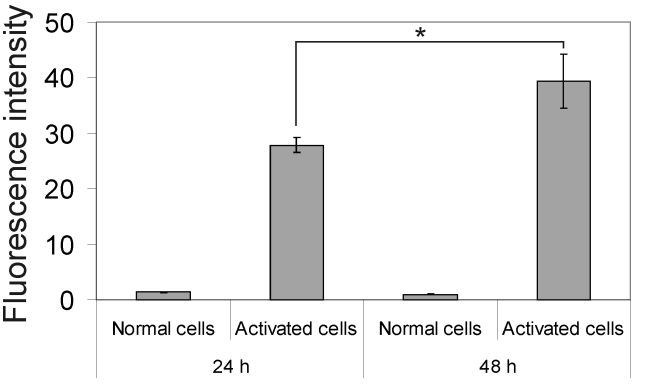

Figure 9. Relative ICAM-1 expression level in A549 cells after activation with TNF-α for 24 and 48 h (* = $p < 0.05$, t test).

TAT-PEG complexes were most stable at a $CaCl_2$ concentration of 75 mM; however, some DNA mobility was observed at most all $CaCl_2$ concentrations (Figure 6B). The stability of 25% TAT-PEG-LABL and 50% TAT-PEG-LABL complexes also depended on $CaCl_2$ concentration. Fifty percent TAT-PEG-LABL complexes started to release DNA at a $CaCl_2$ concentration of 150 mM, and DNA was substantially displaced by heparin at a $CaCl_2$ concentration of 300 mM (Figure 6D).

3.3. Cytotoxicity, Transfection Efficiency, and Intracellular Accumulation of Complexes. Toxicity is a major issue with

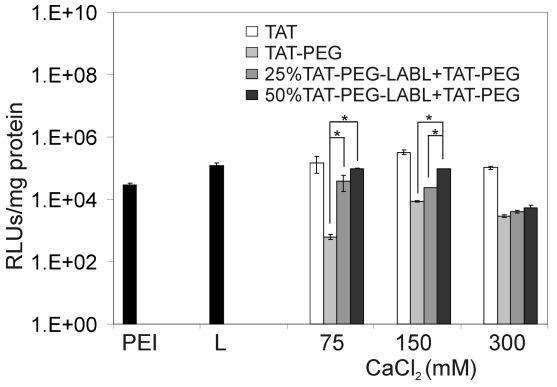

Figure 10. Transfection efficiencies of TAT peptide derivative/DNA complexes in activated A549 cells (overexpressing ICAM-1) at different concentrations of calcium chloride. Complexes were formed at an N/P ratio of 30. L = Lipofectamine (* = $p < 0.05$, one-way ANOVA, Tukey post test).

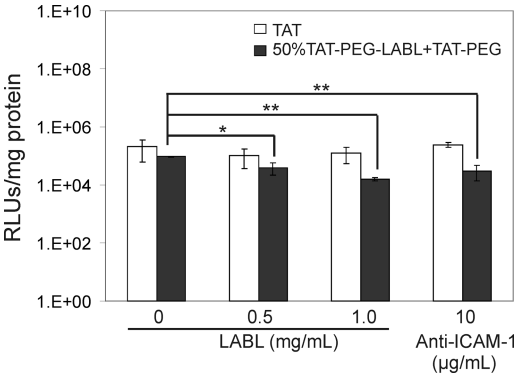

Figure 11. Transfection efficiencies of TAT/DNA and 50% TAT-PEG-LABL/DNA complexes in activated A549 cells (overexpressing ICAM-1) after incubation with free LABL peptide or anti-ICAM-1 mAb prior to exposure to TAT complexes. Complexes were formed at an N/P ratio of 30 and 150 mM $CaCl_2$ (* = $p < 0.05$, ** = $p < 0.01$, one-way ANOVA, Tukey post test).

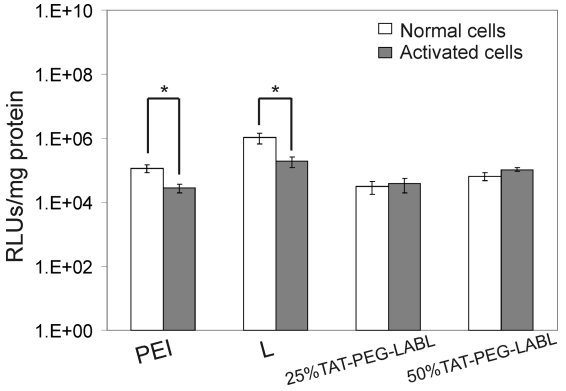

Figure 12. Transfection efficiencies of 25% and 50% TAT-PEG-LABL/DNA complexes in normal and activated A549 cells. Complexes were formed at an N/P ratio of 30 and 150 mM $CaCl_2$ (* = $p < 0.05$, t test).

many nonviral vectors, and a correlation between high toxicity and improved transfection efficiency is often reported.[49] The cytotoxicity of TAT, TAT-PEG, and TAT-PEG-LABL in unactivated and activated A549 cells overexpressing ICAM-1 was evaluated and compared to PEI. After 24 h of incubation, TAT, TAT-PEG, and TAT-PEG-LABL revealed negligible cytotoxicity, whereas PEI showed extreme cytotoxicity with an IC_{50} value of ~50 and ~10 μg/mL in normal and activated cells, respectively (Figure 7). At high concentration, TAT-PEG had slightly less cytotoxicity than TAT in unactivated cells (Figure 7A).

Transfection efficiency was determined in A549 cells. This cell line may be activated by proinflammatory cytokines to overexpress ICAM-1. In order to optimize transfection parameters such as $CaCl_2$ concentration and N/P ratios, transfection studies of TAT/DNA and TAT-PEG/DNA complexes were evaluated in unactivated A549 cells (Figure 8). Luciferase gene expression was measured 48 h post-transfection and compared to PEI and Lipofectamine 2000. Generally, TAT and TAT-PEG complexes showed relatively low transfection efficiencies in the absence of $CaCl_2$ and at low $CaCl_2$ concentrations (e.g., 5 and 30 mM). TAT complexes showed the highest transfection efficiency at 150 mM added $CaCl_2$ (Figure 8A). TAT-PEG complexes showed slightly lower and a similar trend of transfection efficiency compared to TAT complexes. The data suggested that $CaCl_2$ concentrations around 150 mM provided optimal transfection, perhaps due to the small complex size, DNA protection, and/or efficient DNA release.

Next, the transfection efficiencies of TAT and TAT-PEG complexes at different N/P ratios were examined at $CaCl_2$ concentrations of 0, 30, and 75 mM. Using 75 mM of added $CaCl_2$, N/P ratios between 10 and 20 yielded high transfection levels for TAT complexes, exceeding the performance of PEI and Lipofectamine 2000 (Figure 8B). TAT-PEG complexes showed a somewhat similar trend, reaching the maximum transfection level at N/P ~30 and at the highest calcium concentration of 75 mM (Figure 8C). Transfection levels of TAT-PEG complexes were substantially lower than those of TAT complexes, as expected. The reduced transfection level of TAT-PEG was in agreement with complex stability data since TAT-PEG was less effective at packaging DNA (Figure 6B).

Relative ICAM-1 receptor expression levels in A549 cells after activation with TNF-α for 24 and 48 h was quantified using FITC-labeled monoclonal anti-human CD54 (anti-ICAM-1) and a FACscan flow cytometer. The fluorescence intensity representing the relative ICAM-1 expression level showed 22-fold and 41-fold increases in A549 cells after 24 and 48 h of activation compared to normal cells, respectively (Figure 9).

Transfection efficiencies of TAT derivative complexes (e.g., TAT, TAT-PEG, 25% and 50% TAT-PEG-LABL + TAT-PEG) in A549 cells with upregulated ICAM-1 at different concentrations of calcium chloride were examined. Cells were activated with TNF-α for 48 h prior to transfection. Complexes were formed at an N/P ratio of 30, and luciferase gene expression was measured 48 h post-transfection. Overall, complexes formed with 150 mM of added $CaCl_2$ showed superior transfection efficiency compared to complexes formed with other $CaCl_2$ concentrations (Figure 10). Data were consistent with transfection data in normal cells, which showed maximum transfection levels at 75 and 150 mM $CaCl_2$ (Figure 8A). In both normal and activated cells, TAT complexes showed transfection efficiencies (150 mM $CaCl_2$) that were comparable to PEI and Lipofectamine 2000.

As anticipated, TAT-PEG complexes showed the lowest gene expression level; however, transfection efficiency was regained by including targeting ligands (TAT-PEG-LABL) in the formulations. Including 25% TAT-PEG-LABL with TAT-PEG gave

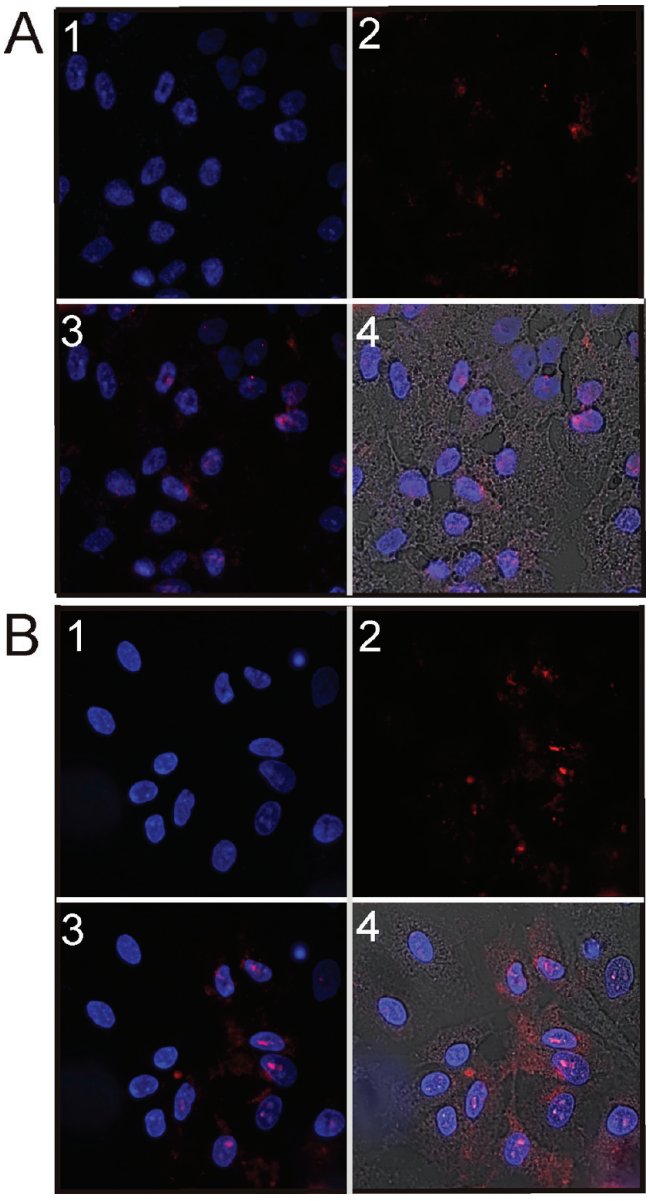

Figure 13. Micrographs of (A) TAT-PEG/DNA complexes and (B) 50% TAT-PEG-LABL/DNA complexes in A549 cells (activated with TNF-α) after 4 h of incubation at 37 °C. Complexes were formed at an N/P ratio of 30 and a $CaCl_2$ of 150 mM (1 = DAPI fluorescence (cell nuclei), 2 = TOTO-3 fluorescence (DNA), 3 = merged DAPI and TOTO-3 fluorescence, 4 = merged DAPI, TOTO-3 fluorescence, and bright field transmission).

improved transfection efficiency compared to TAT-PEG, and 50% TAT-PEG-LABL complexes achieved the highest transfection level for targeted complexes (75 and 150 mM $CaCl_2$). The observed transfection efficiency was consistent with complex size. According to DLS data, complex sizes at 150 mM $CaCl_2$ were small (100−200 nm) and stable in the medium.

A blocking study was performed to determine the effect of ICAM-1 receptor blocking on transfection efficiency of targeted complexes. TAT/DNA and 50% TAT-PEG-LABL/DNA complexes were formed as described earlier at an N/P ratio of 30 using 150 mM $CaCl_2$. Activated cells were incubated with various concentrations of free LABL peptide or anti-ICAM-1 mAb prior to exposure to TAT complexes. The reduced transfection levels of targeted complexes (Figure 11) suggested that the binding of targeted complexes to ICAM-1 on activated A549 cells was hindered when free LABL peptide or anti-ICAM-1 mAb was added. Inhibition was dose dependent with higher LABL concentrations leading to lower transfection. It is worth noting that activated A549 cells exhibited substantially lower transfection when compared to normal cells. Transfection efficiencies of PEI and Lipofectamine 2000 in activated cells were significantly reduced compared to normal cells. Interestingly, 25% and 50% TAT-PEG-LABL complexes were able to maintain transfection levels in both normal and activated cells (Figure 12).

Targeted complexes were expected to enhance binding and internalization compared to untargeted complexes in activated ICAM-1 expressing cells. Untargeted (TAT-PEG) and targeted complexes (50% TAT-PEG-LABL) were imaged by confocal microscopy. DNA was fluorescently labeled using TOTO-3. Both complexes were formed with labeled DNA under the same conditions ($CaCl_2$ 150 mM, N/P = 30) and incubated with activated cells for 4 h. DNA in TAT-PEG complexes was difficult to detect in culture. Conversely, DNA from 50% TAT-PEG-LABL complexes were observed in the vast majority of the cells and overlaid both the cell bodies and nuclei (Figure 13).

4. DISCUSSION

Despite its low molecular weight, TAT was confirmed as a powerful transfection agent when condensed with an optimal concentration of $CaCl_2$. Targeting ligands are expected to improve the performance of these types of vectors when translated to *in vivo* studies. Therefore, TAT was modified with PEG and the peptide LABL, a well-characterized ligand for ICAM-1. TAT, TAT-PEG, and TAT-PEG-LABL block peptides were carefully synthesized and the structure validated. In general, all forms of TAT showed minimal cytotoxicity. TAT-PEG had less cytotoxicity than TAT in unactivated A549 cells. Earlier reports suggest PEGylation often reduces cytotoxicity of cationic polymers.[50,51] The $CaCl_2$ concentration range used in this study was considerably safe. The IC_{50} value of $CaCl_2$ was ∼210 mM for A549 cells.[15] Final concentrations of $CaCl_2$ used with cells in transfection studies ranged from 1 to 60 mM (corresponding to the reported starting concentrations of 5−300 mM), which were far below this IC_{50} value.

TAT and TAT-PEG were able to immobilize DNA starting from N/P ratios 1 and 2, respectively. The data were consistent with previous reports that indicated TAT can immobilize DNA at an N/P ratio as low as ∼2.[15,25] The data also suggested that PEGylation and incorporation of targeting ligand did not interfere with DNA complexation.

Size and morphology of block peptide/DNA complexes were then characterized. Complex stability was also examined using heparin displacement. The data suggested that $CaCl_2$ played a critical role in complex size and DNA release. At optimal $CaCl_2$ concentration (150 mM $CaCl_2$), complexes were small and stable in the medium. It is probable that calcium bridges between DNA phosphate groups and/or TAT amine groups helped condense complexes into compact particles.[15] Ionic strength is known to affect the size of nanoparticle formulations, especially for charged particles. It was reported that adding calcium and magnesium (>30 mM) reduced aggregation and yielded more monodisperse plasmid−lipid nanoparticles.[52]

In addition to controlling particle size, calcium concentration also affected DNA release. For example, 50% TAT-PEG-LABL complexes started to release DNA at a $CaCl_2$ concentration of 150 mM and DNA was substantially displaced by heparin at a $CaCl_2$ concentration of 300 mM (Figure 6D). A previous study suggested that TAT complexes may be "loosened" at high calcium concentration as evidenced by fluorescent DNA probes.[15] Ionic strength may also contribute to the observed destabilization. It has been reported that, at low salt concentration ($\leq$50 mM NaCl), polymer−DNA binding is not strongly dependent on ionic strength. High salt concentration, however, can alter polymer−DNA binding and may cause dissociation of complexes due to electrostatic shielding.[53] The stability of polycation/DNA complexes has been identified as a rate limiting step for intracellular release of DNA, which can impair transfection efficiency. Previous reports showed "weak" chitosan polyplexes offered a faster onset of transfection and higher gene expression both *in vitro* and *in vivo*.[54] Therefore, a fine balance between complex stability and DNA release is essential for efficient transfection. Tuning calcium concentration provides a simple formulation approach for optimizing TAT complex size and DNA release.

Transfection efficiencies of TAT and TAT-PEG in A549 cells were enhanced by optimizing calcium concentration. The data suggested that small complex size, optimal complex stability and DNA release may contribute to the improved gene expression. Calcium has been shown to enhance transfection efficiency for lipid gene delivery systems.[52,55−57] The detailed mechanism of calcium enhancement for these systems has not been clear, and several mechanisms have been proposed.[52,56,57] It was suggested that calcium may increase membrane association or cellular uptake of complexes or particles. More importantly, calcium may act as a lysosomotropic agent and destabilize endosomal and/or lysosomal membranes thus increasing endolysosomal release. Interestingly, Fujita and others reported that calcium did not improve the performance of arginine-PEG-lipid-coated DNA/protamine complexes.[55] Generally, substantially higher calcium concentrations were used to condense and control DNA release from modified TAT complexes reported here.

Several groups have used TAT peptides at high N/P ratios possibly because TAT peptides have also been shown to lose membrane translocation ability upon binding to DNA.[25,58] It was reported that excess free TAT peptides enhanced transfection efficiency of TAT/DNA complexes by preventing complex disruption by proteoglycans.[59] Interestingly, it was also previously reported that large amounts of free PEI remained in PEI/DNA mixtures. The presence of free PEI was suggested to improve membrane permeability, thus enhancing DNA release into the cytoplasm.[60]

Adding the PEG block served as a hydrophilic arm for attaching targeting ligands with the goal of recovering transfection efficiency and adding specificity. LABL, a peptide ligand for ICAM-1, was linked to TAT-PEG using solid phase synthesis. The resulting TAT-PEG-LABL was confirmed using mass spectrometry (Figure 2), and used in studies with actived A549 cells, which overexpress ICAM-1 . TAT-PEG-LABL and TAT-PEG were mixed at different ratios resulting in a different percentage of targeting ligands when forming complexes with DNA. This targeted gene delivery system was then explored for transfection of A549 cells overexpressing ICAM-1. PEGylation significantly reduced transfection efficiency when compared to unmodified TAT as expected. The low transfection observed for TAT-PEG complexes was consistent with poor complex stability and with previous reports that indicated PEG-based polymers or liposomes had reduced transfection levels, possibly due to steric hindrance.[18,53] Transfection efficiency was recovered by incorporating the LABL targeting ligand.

Complexes containing 50% TAT-PEG-LABL 75 and 150 mM showed high transfection levels when 75 and 150 mM $CaCl_2$ was added. The relatively low transfection efficiencies of 25% and 50% TAT-PEG-LABL complexes at 300 mM $CaCl_2$ may be due to their large sizes (430 and ~900 nm, respectively) in the medium and inadequate ability to protect DNA as suggested by heparin displacement data. It was previously reported that particles smaller than ~200 nm were internalized mainly by endocytosis, whereas particles larger than ~200 nm were taken up mostly by phagocytosis.[61] It was also reported that, when phagocytosis occurs, transfection efficiency can be reduced.[16] The blocking data strongly supported a specific, ICAM-1 receptor mediated interaction.

PEI and Lipofectamine 2000 showed significantly reduced transfection levels in activated cells compared to normal cells. Exposure to TNF-α, a proinflammatory cytokine, can alter cellular functions. Previous reports showed that TNF-α decreased cell viability in primary and immortalized cell lines.[62,63] Some studies have also shown that, under inflammatory conditions, cells often have decreased endocytic activity and different endocytic pathways may be favored.[64] This is important evidence that certain cell types may be more difficult to transfect due to abnormal cellular functions under pathological conditions.

The observed transfection efficiency of targeted complexes resulted from a combination of optimal complex size, complex stability, DNA release, and the presence of targeting ligands. These characteristics are well-known to effect internalization and DNA release, and the resulting transfection efficiency. The performance of targeted TAT-PEG-LABL suggested that these complexes may be a promising vector for targeted gene transfection to sites of inflammation *in vivo*. Although accurate targeting of TAT-PEG-LABL complexes was demonstrated here, it may be necessary to investigate other epithelial, endothelial, or inflammatory cell lines.

AUTHOR INFORMATION

Corresponding Author

*University of Kansas, Department of Pharmaceutical Chemistry, 2030 Becker Drive, Lawrence, Kansas 66047. Phone: (785) 864-1455. Fax: (785) 864-1454. E-mail: berkland@ku.edu.

ACKNOWLEDGMENT

The authors are grateful to Dr. David Moore and Heather Shinogle (Microscopy and analytical imaging laboratories) for their generous assistance in imaging and to Prof. Russell Middaugh for the use of laboratory equipment. Additionally, we would like to acknowledge support from Naresuan University, Thailand. Also, lab support from the Coulter Foundation, the NIH (R03 AR054035, P20 RR016443), and the Institute for Advancing Medical Innovation.

REFERENCES

(1) Russ, V.; Wagner, E. Cell and tissue targeting of nucleic acids for cancer gene therapy. *Pharm. Res.* **2007**, *24* (6), 1047–1057.

(2) Li, S. D.; Huang, L. Gene therapy progress and prospects: non-viral gene therapy by systemic delivery. *Gene Ther.* **2006**, *13* (18), 1313–1319.

(3) Kirschberg, T. A.; VanDeusen, C. L.; Rothbard, J. B.; Yang, M.; Wender, P. A. Arginine-based molecular transporters: the synthesis and chemical evaluation of releasable taxol-transporter conjugates. *Org. Lett.* **2003**, *5* (19), 3459–3462.

(4) Rothbard, J. B.; Garlington, S.; Lin, Q.; Kirschberg, T.; Kreider, E.; McGrane, P. L.; Wender, P. A.; Khavari, P. A. Conjugation of arginine oligomers to cyclosporin A facilitates topical delivery and inhibition of inflammation. *Nat. Med.* **2000**, *6* (11), 1253–1257.

(5) Bhorade, R.; Weissleder, R.; Nakakoshi, T.; Moore, A.; Tung, C. H. Macrocyclic chelators with paramagnetic cations are internalized into mammalian cells via a HIV-tat derived membrane translocation peptide. *Bioconjugate Chem.* **2000**, *11* (3), 301–305.

(6) Kersemans, V.; Kersemans, K.; Cornelissen, B. Cell penetrating peptides for in vivo molecular imaging applications. *Curr. Pharm. Des.* **2008**, *14* (24), 2415–2427.

(7) Corradin, S.; Ransijn, A.; Corradin, G.; Bouvier, J.; Delgado, M. B.; Fernandez-Carneado, J.; Mottram, J. C.; Vergères, G.; Mauël, J. Novel peptide inhibitors of Leishmania gp63 based on the cleavage site of MARCKS (myristoylated alanine-rich C kinase substrate)-related protein. *Biochem. J.* **2002**, *367* (Part 3), 761.

(8) Datta, K.; Sundberg, C.; Karumanchi, S. A.; Mukhopadhyay, D. The 104−123 Amino Acid Sequence of the {beta}-domain of von Hippel-Lindau Gene Product Is Sufficient to Inhibit Renal Tumor Growth and Invasion. *Cancer Res.* **2001**, *61* (5), 1768.

(9) Fawell, S.; Seery, J.; Daikh, Y.; Moore, C.; Chen, L. L.; Pepinsky, B.; Barsoum, J. Tat-mediated delivery of heterologous proteins into cells. *Proc. Natl. Acad. Sci. U.S.A.* **1994**, *91* (2), 664.

(10) Wadia, J.; Dowdy, S. Transmembrane delivery of protein and peptide drugs by TAT-mediated transduction in the treatment of cancer. *Adv. Drug Delivery Rev.* **2005**, *57* (4), 579–596.

(11) Eguchi, A.; Akuta, T.; Okuyama, H.; Senda, T.; Yokoi, H.; Inokuchi, H.; Fujita, S.; Hayakawa, T.; Takeda, K.; Hasegawa, M. Protein transduction domain of HIV-1 Tat protein promotes efficient delivery of DNA into mammalian cells. *J. Biol. Chem.* **2001**, *276* (28), 26204.

(12) Snyder, E. L.; Dowdy, S. F. Protein/peptide transduction domains: potential to deliver large DNA molecules into cells. *Curr. Opin. Mol. Ther.* **2001**, *3* (2), 147.

(13) Jesus, M.; Berry, C. C. Tat peptide as an efficient molecule to translocate gold nanoparticles into the cell nucleus. *Bioconjugate Chem.* **2005**, *16* (5), 1176–1180.

(14) Sethuraman, V. A.; Bae, Y. H. TAT peptide-based micelle system for potential active targeting of anti-cancer agents to acidic solid tumors. *J. Controlled Release* **2007**, *118* (2), 216–224.

(15) Baoum, A.; Xie, S.; Fakhari, A.; Berkland, C. Soft" Calcium Crosslinks Enable Highly Efficient Gene Transfection Using TAT Peptide. *Pharm. Res.* **2009**, *26* (12), 2619–2629.

(16) Pedraza, C. E.; Bassett, D. C.; McKee, M. D.; Nelea, V.; Gbureck, U.; Barralet, J. E. The importance of particle size and DNA condensation salt for calcium phosphate nanoparticle transfection. *Biomaterials* **2008**, *29* (23), 3384.

(17) Josephson, L.; Tung, C.; Moore, A.; Weissleder, R. High-efficiency intracellular magnetic labeling with novel superparamagnetic-Tat peptide conjugates. *Bioconjugate Chem.* **1999**, *10* (2), 186–191.

(18) Kale, A.; Torchilin, V. Enhanced transfection of tumor cells in vivo using "Smart" pH-sensitive TAT-modified pegylated liposomes. *J. Drug Targeting* **2007**, *15* (7), 538–545.

(19) MacKay, J.; Li, W.; Huang, Z.; Dy, E.; Huynh, G.; Tihan, T.; Collins, R.; Deen, D.; Szoka, F., Jr. HIV TAT peptide modifies the distribution of DNA nanolipoparticles following convection-enhanced delivery. *Mol. Ther.* **2008**, *16* (5), 893–900.

(20) Moschos, S.; Williams, A.; Lindsay, M. Cell-penetrating-peptide-mediated siRNA lung delivery. *Biochem. Soc. Trans.* **2007**, *35*, 807–810.

(21) Pappalardo, J.; Quattrocchi, V.; Langellotti, C.; Di Giacomo, S.; Gnazzo, V.; Olivera, V.; Calamante, G.; Zamorano, P.; Levchenko, T.; Torchilin, V. Improved transfection of spleen-derived antigen-presenting cells in culture using TATp-liposomes. *J. Controlled Release* **2009**, *134* (1), 41–46.

(22) Suk, J.; Suh, J.; Choy, K.; Lai, S.; Fu, J.; Hanes, J. Gene delivery to differentiated neurotypic cells with RGD and HIV Tat peptide functionalized polymeric nanoparticles. *Biomaterials* **2006**, *27* (29), 5143–5150.

(23) Manickam, S. Influence of TAT-peptide polymerization on properties and transfection activity of TAT/DNA polyplexes. *J. Controlled Release* **2005**, *102* (1), 293–306.

(24) Reschel, T. Physical properties and in vitro transfection efficiency of gene delivery vectors based on complexes of DNA with synthetic polycations. *J. Controlled Release* **2002**, *81* (1−2), 201–217.

(25) Rudolph, C.; Plank, C.; Lausier, J.; Schillinger, U.; M ller, R.; Rosenecker, J. Oligomers of the arginine-rich motif of the HIV-1 TAT protein are capable of transferring plasmid DNA into cells. *J. Biol. Chem.* **2003**, *278* (13), 11411.

(26) Rudolph, C.; Schillinger, U.; Ortiz, A.; Tabatt, K.; Plank, C.; M ller, R.; Rosenecker, J. Application of novel solid lipid nanoparticle (SLN)-gene vector formulations based on a dimeric HIV-1 TAT-peptide in vitro and in vivo. *Pharm. Res.* **2004**, *21* (9), 1662–1669.

(27) Hersmann, G. H. W.; Kriegsmann, J.; Simon, J.; Hüttich, C.; Bräuer, R. Expression of cell adhesion molecules and cytokines in murine antigen-induced arthritis. *Cell Commun. Adhes.* **1998**, *6* (1), 69–82.

(28) Swerlick, R. A.; Garcia-Gonzalez, E.; Kubota, Y.; Xu, Y.; Lawley, T. J. Studies of the Modulation of MHC Antigen and Cell Adhesion Molecule Expression on Human Dermal Microvascular Endotheliam Cells. *J. Invest. Dermatol.* **1991**, *97* (2), 190–196.

(29) Zecchinon, L.; Fett, T.; Vanden Bergh, P.; Desmecht, D. Bind another day: The LFA-1/ICAM-1 interaction as therapeutic target. *Clin. Appl. Immunol. Rev.* **2006**, *6* (3−4), 173–189.

(30) Bevilacqua, M. P.; Nelson, R. M.; Mannori, G.; Cecconi, O. Endothelial-leukocyte adhesion molecules in human disease. *Annu. Rev. Med.* **1994**, *45* (1), 361–378.

(31) Melis, M.; Spatafora, M.; Melodia, A.; Pace, E.; Gjomarkaj, M.; Merendino, A. M.; Bonsignore, G. ICAM-1 expression by lung cancer cell lines: effects of upregulation by cytokines on the interaction with LAK cells. *Eur. Respir. J.* **1996**, *9* (9), 1831.

(32) Chittasupho, C.; Xie, S. X.; Baoum, A.; Yakovleva, T.; Siahaan, T. J.; Berkland, C. J. ICAM-1 targeting of doxorubicin-loaded PLGA nanoparticles to lung epithelial cells. *Eur. J. Pharm. Sci.* **2009**, *37* (2), 141–150.

(33) Yacyshyn, B. R.; Chey, W. Y.; Goff, J.; Salzberg, B.; Baerg, R.; Buchman, A. L.; Tami, J.; Yu, R.; Gibiansky, E.; Shanahan, W. R. Double blind, placebo controlled trial of the remission inducing and steroid sparing properties of an ICAM-1 antisense oligodeoxynucleotide, alicaforsen (ISIS 2302), in active steroid dependent Crohn's disease. *Gut* **2002**, *51* (1), 30.

(34) Weller, G. E. R.; Villanueva, F. S.; Tom, E. M.; Wagner, W. R. Targeted ultrasound contrast agents: in vitro assessment of endothelial dysfunction and multi-targeting to ICAM-1 and sialyl Lewisx. *Biotechnol. Bioeng.* **2005**, *92* (6), 780–788.

(35) Demos, S. M.; Alkan-Onyuksel, H.; Kane, B. J.; Ramani, K.; Nagaraj, A.; Greene, R.; Klegerman, M.; McPherson, D. D. In vivo targeting of acoustically reflective liposomes for intravascular and transvascular ultrasonic enhancement. *J. Am. Coll. Cardiol.* **1999**, *33* (3), 867–875.

(36) Muro, S.; Cui, X.; Gajewski, C.; Murciano, J. C.; Muzykantov, V. R.; Koval, M. Slow intracellular trafficking of catalase nanoparticles targeted to ICAM-1 protects endothelial cells from oxidative stress. *Am. J. Physiol.* **2003**, *285* (5), C1339.

(37) Murciano, J. C.; Muro, S.; Koniaris, L.; Christofidou-Solomidou, M.; Harshaw, D. W.; Albelda, S. M.; Granger, D. N.; Cines, D. B.; Muzykantov, V. R. ICAM-directed vascular immunotargeting of antithrombotic agents to the endothelial luminal surface. *Blood* **2003**, *101* (10), 3977.

(38) Scherpereel, A.; Wiewrodt, R.; Christofidou-Solomidou, M.; Gervais, R.; Murciano, J. C.; Albelda, S. M.; Muzykantov, V. R. Cell-selective

intracellular delivery of a foreign enzyme to endothelium in vivo using vascular immunotargeting. *FASEB J.* **2001**, *15* (2), 416.

(39) Yusuf-Makagiansar, H.; Yakovleva, T. V.; Tejo, B. A.; Jones, K.; Hu, Y.; Verkhivker, G. M.; Audus, K. L.; Siahaan, T. J. Sequence Recognition of -LFA-1-derived Peptides by ICAM-1 Cell Receptors: Inhibitors of T-cell Adhesion. *Chem. Biol. Drug Des.* **2007**, *70* (3), 237–246.

(40) Anderson, M. E.; Siahaan, T. J. Targeting ICAM-1/LFA-1 interaction for controlling autoimmune diseases: designing peptide and small molecule inhibitors. *Peptides* **2003**, *24* (3), 487.

(41) Zhao, H.; Kiptoo, P.; Williams, T.; Siahaan, T.; Topp, E. Immune response to controlled release of immunomodulating peptides in a murine experimental autoimmune encephalomyelitis (EAE) model. *J. Controlled Release* **2009**.

(42) Yonekawa, K.; Harlan, J. Targeting leukocyte integrins in human diseases. *J. Leukocyte Biol.* **2005**, *77* (2), 129.

(43) Yusuf-Makagiansar, H.; Siahaan, T. Binding and internalization of an LFA-1-derived cyclic peptide by ICAM receptors on activated lymphocyte: a potential ligand for drug targeting to ICAM-1-expressing cells. *Pharm. Res.* **2001**, *18* (3), 329–335.

(44) Konno, S.; Grindle, K.; Lee, W.; Schroth, M.; Mosser, A.; Brockman-Schneider, R.; Busse, W.; Gern, J. Interferon-gamma enhances rhinovirus-induced RANTES secretion by airway epithelial cells. *Am. J. Respir. Cell Mol. Biol.* **2002**, *26* (5), 594.

(45) Fakhari, A; Baoum, A; Siahaan, T. J.; Le, K. B.; Berkland, C. Controlling Ligand Surface Density Optimizes Nanoparticle Binding to ICAM-1. *J. Pharm. Sci.* **2010**, *100* (3), 1045–1056.

(46) Mansouri, S.; Lavigne, P.; Corsi, K.; Benderdour, M.; Beaumont, E.; Fernandes, J. Chitosan-DNA nanoparticles as non-viral vectors in gene therapy: strategies to improve transfection efficacy. *Eur. J. Pharm. Biopharm.* **2004**, *57* (1), 1–8.

(47) Veronese, F.; Pasut, G. PEGylation, successful approach to drug delivery. *Drug Discovery Today* **2005**, *10* (21), 1451–1458.

(48) Won, Y.; Sharma, R.; Konieczny, S. Missing pieces in understanding the intracellular trafficking of polycation/DNA complexes. *J. Controlled Release* **2009**, *139*, 88–93.

(49) Godbey, W.; Wu, K.; Mikos, A. Poly (ethylenimine)-mediated gene delivery affects endothelial cell function and viability. *Biomaterials* **2001**, *22* (5), 471–480.

(50) Beyerle, A.; Merkel, O.; Stoeger, T.; Kissel, T. PEGylation affects cytotoxicity and cell-compatibility of poly (ethylene imine) for lung application: Structure-function relationships. *Toxicol. Appl. Pharmacol.* **2010**, *242* (2), 146–154.

(51) Zhang, X.; Pan, S.; Hu, H.; Wu, G.; Feng, M.; Zhang, W.; Luo, X. Poly (ethylene glycol)-block-polyethylenimine copolymers as carriers for gene delivery: Effects of PEG molecular weight and PEGylation degree. *J. Biomed. Mater. Res., Part A* **2007**, *84* (3), 795–804.

(52) Palmer, L.; Chen, T.; Lam, A.; Fenske, D.; Wong, K.; MacLachlan, I.; Cullis, P. Transfection properties of stabilized plasmid-lipid particles containing cationic PEG lipids. *Biochim. Biophys. Acta, Biomembranes* **2003**, *1611* (1−2), 204–216.

(53) Rungsardthong, U.; Deshpande, M.; Bailey, L.; Vamvakaki, M.; Armes, S. P.; Garnett, M. C.; Stolnik, S. Copolymers of amine methacrylate with poly (ethylene glycol) as vectors for gene therapy. *J. Controlled Release* **2001**, *73* (2−3), 359–380.

(54) Köping-Höggård, M.; Vårum, K. M.; Issa, M.; Danielsen, S.; Christensen, B. E.; Stokke, B. T.; Artursson, P. Improved chitosan-mediated gene delivery based on easily dissociated chitosan polyplexes of highly defined chitosan oligomers. *Gene Ther.* **2004**, *11* (19), 1441–1452.

(55) Fujita, T.; Furuhata, M.; Hattori, Y.; Kawakami, H.; Toma, K.; Maitani, Y. Calcium enhanced delivery of tetraarginine-PEG-lipid-coated DNA/protamine complexes. *Int. J. Pharm.* **2009**, *368* (1−2), 186–192.

(56) Sandhu, A.; Lam, A.; Fenske, D.; Palmer, L.; Johnston, M.; Cullis, P. Calcium enhances the transfection potency of stabilized plasmid-lipid particles. *Anal. Biochem.* **2005**, *341* (1), 156–164.

(57) Shiraishi, T.; Pankratova, S.; Nielsen, P. Calcium ions effectively enhance the effect of antisense peptide nucleic acids conjugated to cationic tat and oligoarginine peptides. *Chem. Biol.* **2005**, *12* (8), 923–929.

(58) Liu, Z.; Li, M.; Cui, D.; Fei, J. Macro-branched cell-penetrating peptide design for gene delivery. *J. Controlled Release* **2005**, *102* (3), 699–710.

(59) Ignatovich, I.; Dizhe, E.; Pavlotskaya, A.; Akifiev, B.; Burov, S.; Orlov, S.; Perevozchikov, A. Complexes of plasmid DNA with basic domain 47−57 of the HIV-1 Tat protein are transferred to mammalian cells by endocytosis-mediated pathways. *J. Biol. Chem.* **2003**, *278* (43), 42625.

(60) Moghimi, S.; Symonds, P.; Murray, J.; Hunter, A.; Debska, G.; Szewczyk, A. A two-stage poly (ethylenimine)-mediated cytotoxicity: implications for gene transfer/therapy. *Mol. Ther.* **2005**, *11* (6), 990–995.

(61) Xiang, S. D.; Scholzen, A.; Minigo, G.; David, C.; Apostolopoulos, V.; Mottram, P. L.; Plebanski, M. Pathogen recognition and development of particulate vaccines: does size matter? *Methods* **2006**, *40* (1), 1–9.

(62) Beg, A.; Baltimore, D. An essential role for NF-kappa B in preventing TNF-alpha-induced cell death. *Science* **1996**, *274* (5288), 782.

(63) Li, L.; Thomas, R.; Suzuki, H.; De Brabander, J.; Wang, X.; Harran, P. A small molecule Smac mimic potentiates TRAIL-and TNF {alpha}-mediated cell death. *Science* **2004**, *305* (5689), 1471.

(64) Foerg, C.; Merkle, H. P. On the biomedical promise of cell penetrating peptides: limits versus prospects. *J. Pharm. Sci.* **2007**, *97* (1), 144–162.